



Article

Plasma-Activated Polyvinyl Alcohol Foils for Cell Growth

Nikola Slepíčková Kasálková ¹, Petr Slepíčka ^{1,*}, Barbora Ivanovská ¹, Martina Trávníčková ², Petr Malinský ³, Anna Macková ³ , Lucie Bačáková ²  and Václav Švorčík ¹

¹ Department of Solid State Engineering, University of Chemistry and Technology Prague, 166 28 Prague, Czech Republic; nikola.kasalkova@vscht.cz (N.S.K.); barbora.ivanovska@vscht.cz (B.I.); vaclav.svorcik@vscht.cz (V.Š.)

² Department of Biomaterials and Tissue Engineering, Institute of Physiology of the Czech Academy of Sciences, Vídeňská 1083, 14220 Prague, Czech Republic; Martina.Travnickova@fgu.cas.cz (M.T.); Lucie.Bacakova@fgu.cas.cz (L.B.)

³ Department of Neutron Physics, Nuclear Physics Institute of the Czech Academy of Sciences, 25068 Řež, Czech Republic; malinsky@ujf.cas.cz (P.M.); mackova@ujf.cas.cz (A.M.)

* Correspondence: petr.slepicka@vscht.cz; Tel.: +42-0220-445-162

Received: 23 October 2020; Accepted: 9 November 2020; Published: 11 November 2020



Abstract: Hydrogels, and not only natural polysaccharide hydrogels, are substances capable of absorbing large amounts of water and physiological fluids. In this study, we set out to optimize the process for preparing polyvinyl alcohol (PVA) hydrogels. Subsequently, we doped PVA foils with cellulose powder, with poly(ethylene glycol) (PEG) or with gold nanoparticles in PEG colloid solutions (Au). The foils were then modified in a plasma discharge to improve their biocompatibility. The properties of PVA foils were studied by various analytical methods. The use of a suitable dopant can significantly affect the surface wettability, the roughness, the morphology and the mechanical properties of the material. Plasma treatment of PVA leads to ultraviolet light-induced crosslinking and decreasing water absorption. At the same time, this treatment significantly improves the cytocompatibility of the polymer, which is manifested by enhanced growth of human adipose-derived stem cells. This positive effect on the cell behavior was most pronounced on PVA foils doped with PEG or with Au. This modification of PVA therefore seems to be most suitable for the use of this polymer as a cell carrier for tissue engineering, wound healing and other regenerative applications.

Keywords: cytocompatibility; nanoparticle doping; plasma treatment; polymer; PVA; surface characterization; tissue engineering

1. Introduction

Advances in cellular and molecular biology, chemistry and material engineering have provided much greater opportunities for the clinical use of biomaterials. These technologies still involve the use of common materials such as metals, ceramics and synthetic polymers, but must be complemented by being combined with advanced materials such as biopolymers, nanoparticles or carbon nanotubes [1]. Areas of research and also innovative technologies, such as drug delivery systems and imaging methods based on nanotechnology or on organ printing, are based on the use of biomaterials. There are a number of key factors to consider when designing, synthesizing or determining the suitability of a tissue engineered scaffold, e.g., biocompatibility, biodegradability, mechanical properties, porosity, etc. [2–4].

Hydrogels are three-dimensional hydrophilic polymeric structures with the ability to absorb large amounts of water or biological fluids [5]. The hydrophilic nature of the network is due to the presence

of hydrophilic groups in the polymeric structure, i.e., hydroxyl (–OH), carboxyl (–COOH), amide (–CONH–) or sulfone (–SO₃H) groups, among others. The presence of these functional groups is essential for later crosslinking [6,7]. The ability of hydrogels to absorb water and physiological fluids leads to improved biocompatibility and biodegradability of these materials. The elastomeric nature of hydrogels helps to ensure minimal mechanical damage to surrounding tissues, and their ability to swell results in high permeability for low molecular weight drug molecules. Due to their unique properties, hydrogels are increasingly used in the field of biomedical applications as wound covers, carriers for controlled drug delivery, substrates for the fabrication of contact lenses, substrates for tissue engineering using stem cells, or for engineering blood-contacting prosthetic devices [8,9]. Three-dimensional networks are formed by polymerizing one or more types of monomers and by subsequent crosslinking of polymer chains, which prevent the dissolution of hydrogels in water [6,10,11]. The character of the water component in a hydrogel can determine the overall permeation of nutrients into cells and of cellular products into the gel. When a dry hydrogel begins to absorb water, the first water molecules entering the matrix hydrate the most polar, hydrophilic groups, leading to “primary bound water”. As the polar groups are hydrated, the network swells, and this exposes hydrophobic groups, which also interact with water molecules, leading to hydrophobically-bound water, or “secondary bound water”. Primary and secondary bound water are often combined, and are simply referred to as the “total bound water” [6].

Although the mechanical properties of hydrogels are to some extent influenced by the water content, they mainly depend on the degree of crosslinking of the polymer chains. This crosslinking changes the physical and chemical structure of the polymer [12]. If the crosslinking is low, the elastic behavior of the material prevails. However, when the crosslinking of the chains is high, the elasticity is reduced and the material undergoes almost no deformation. The relatively easy deformation and the ability to adapt to the shape of the surface make hydrogels promising mucoadhesive dressings, i.e., materials capable of adhering to the slime layer covering the mucosal epithelium. The ability of a hydrogel to adhere to the skin in a fully swollen state is an important advantage, provided that complete, easy and painless removal is possible [13]. Among others, hydrogels have the ability to mimic the mechanical behavior of the extracellular matrix (ECM) in soft tissues [14].

Tissue regeneration is accompanied by a number of overlapping phases, ranging from inflammation, cell migration and proliferation to cell maturation. In the initial phase of wound healing, a sterile environment is required. This is followed by secretion of growth factors into the wound exudates, and by migration of epithelial cells (i.e., keratinocytes) and fibroblasts to the damaged area in order to regenerate the damaged tissue. In the next phase, during proliferation, the wound closes and the layer of epithelial cells on the damaged skin recovers [15]. Numerous dressing materials in the form of foils, foams, semipermeable adhesive films, or hydrogels have been developed on the basis of wound types and healing models. The hydrogel coating creates a humid environment, allows the gas exchange that is necessary for tissue renewal, serves as a barrier to microorganisms, is easy to replace, and exhibits high biocompatibility. In addition, the dressing is usually transparent, allowing wound healing to be monitored [16,17].

Hydrogels may be used for all stages of wound healing except for infected wounds or wounds where the exudate is abundant. The effectiveness of hydrogels in wound healing can be improved by incorporating drugs, growth factors or biologically active substances into the structure of these materials [18]. Hydrogels, and also other types of polymers with incorporated nanoparticles, such as carbon, polymer, inorganic or organic nanoparticles, are called nanocomposite hydrogels. These nanoparticles, incorporated into the surface layer or into the entire volume of the polymer, interact physically or covalently with polymer chains to form a nanocomposite network with novel surface properties or cytocompatibility [19,20]. Some metal nanoparticles or nanolayers (e.g., Ag) exhibit antimicrobial effects [21], and can therefore be used in drug delivery systems. The ability to stimulate the chemical, mechanical, electrical and biological properties of a tissue make them promising candidates in tissue engineering and in constructing novel biomaterials [22].

Polyvinyl alcohol (PVA) is a water-soluble, synthetic, thermoplastic polymer that is used in industrial, food and medical technologies [23,24]. It is used in the chemical industry as a thickener for paints, and also in the production of oil-resistant adhesives and impregnates. Partially hydrolyzed PVA is used in the food industry, where it is applied as a moisture barrier for food supplements, or generally for foods that need to be protected from humidity [25]. Biocompatibility, low protein adsorption, high water solubility and high chemical resistance are features that make PVA useful in biomedical applications in the form of soft contact lenses, eye drops, surgical barriers to tissue adhesion, or artificial cartilage and meniscus [26]. In general, the physical and chemical properties of hydrogels, such as water solubility, diffusivity, crystallinity, wettability, biodegradability, adhesion, or mechanical strength, are influenced by the parameters mentioned above, and are properties to be considered during the preparation of hydrogels and other polymeric materials for biomedical application [27,28]. Unmodified PVA foils are unstable in water, and this may damage the foil. Damage can be prevented by crosslinking PVA, which forms a network for trapping suitable biomolecules. The main techniques used to form water insoluble networks are based on thermal, physical or chemical processes [29].

Thermal treatment of PVA results in a spatial rearrangement of the polymer chains and in the formation of stronger hydrogen bonds between the hydroxyl groups, leading to an increase in the crystalline fraction. The physical ageing of aqueous PVA solutions can lead to partial crosslinking of PVA, because the chains can become entangled together. The chemically cross-linked films are based on the reaction between the crosslinking agent and the big amount of hydroxyl groups in the PVA molecules. There is a wide variety of crosslinking agents for PVA, such as maleic acid, formaldehyde, and glutaraldehyde. Whether intermolecular or intramolecular reactions predominate can be controlled by the reagents that are used, or by changing the operating conditions. The crosslinking mechanism that is chosen can affect both the mechanical strength and the hydrophilic character of the newly-formed membranes [29–33]. The physical method realized by means of plasma radiation can also be used for crosslinking. For a whole range of polymers, plasma treatment leads to a change in surface parameters, to nanostructuring of the surface, or to a change in the biocompatibility of the material [34,35]. In the case of hydrogels, it can therefore be assumed that plasma modification will not only lead to crosslinking, but will also affect surface properties such as morphology, roughness, wettability, and also cell–substrate interactions.

Glutaraldehyde crosslinking does not require heat treatment; among other things, glutaraldehyde has the ability to bind non-specifically to biomolecules such as proteins. The crosslinking agent has two active sites that can be successfully used for simultaneous binding of a protein and PVA. This attribute allows the development of structures that find use as biosensors. A commonly-used process for crosslinking PVA with glutaraldehyde is to immerse the film in an alcohol solution containing a crosslinking agent and an acid, either hydrochloric acid or sulfuric acid. The alcohol medium helps to enlarge the PVA membrane, which facilitates the diffusion of dialdehyde molecules and proton ions that catalyze the reaction [29]. However, the main disadvantage of glutaraldehyde lies in its toxicity, even at low concentrations—there is a risk of leaching of toxic residues and subsequent inhibition of cell growth. For this reason, the use of glutaraldehyde in medical or pharmaceutical applications is limited, and other methods for efficiently crosslinking PVA are being investigated [36]. Since most of the chemical cross-linkers used exhibit some degree of toxicity, citric acid appears to be a more appropriate agent. It is a non-toxic hydroxyl-containing polycarboxylic acid. This acid allows the formation of hydrogen bonds and crosslinking of PVA through an esterification reaction. Very interesting studies on polymer composites involving their applications as scaffolds for tissue engineering or as materials for electronics have been published by the Bismarck group [37–39].

Among the various hydrogels described in literature, hydrogels prepared using PVA blended with some natural polysaccharides and some other synthetic ones are attractive and the most widespread route of their synthesis. Properties of hydrogels based PVA-composite polymers have outperformed their counterparts of other polymers [18,40]. By adding dopants such as poly(ethylene glycol) (PEG) or cellulose (Cel), we can positively affect and significantly improve the biocompatibility, biological

characteristics (no inhibition for cells proliferation), and wound healing size and rate, but also the thermal stability and mechanical properties of materials, or we can also improve their functionality (tableability, compressibility . . .) [18,41].

PVA hydrogels are modified for improving of mechanical and physicochemical properties by addition of other polymeric materials and substances. PVA hydrogel can be modified by adding, e.g., glucan, dextran, starch or gelatine for wound dressing applications, Ag nanoparticles or nanofibers for forming bacterial growth inhibiting materials [40], or amino acid (e.g., glycine, lysine or phenyl alanine) for the tuning of surface characteristics as well as to instigate both osteointegration and antibacterial activity [42]. Blending PVA with chitosan leads to increased swelling capacity, water vapor transmission, and pore area. On the contrary, it can decrease the mechanical and thermal stability of membranes [18]. Blending PVA with biomacromolecules, such as fibronectin, chitosan or heparin, is very attractive because these components have intrinsic biological properties which should be beneficial for cell adhesion and proliferation [43]. Swelling and reswelling properties of PVA can be improved by blending PVA with a certain ratio of crosslinking polymer [12].

The properties of PVA hydrogels can be modified not only by adding “new compounds” but also by adjusting the amount (ratio) of the raw materials used in their production. Polymer swelling can be accomplished by modifying the conditions of its preparation, including crosslinking content [12].

The second way to modify PVA hydrogels and modify their properties is the physical method. A novel plasma-assisted bioprinting system allows the processing of soft hard biomaterial integration and plasma surface modification layer by layer during the fabrication process in the same chamber. The plasma-assisted bio-extrusion system (PABS) was used to produce PCL/Hydrogel hybrid scaffolds and plasma fully treated scaffolds [44]. Using low pressure plasma leads to the introduction of OKdifferent functional groups and to the anchorage of “other” substances and compounds containing on polymer surfaces [45].

Another possible application of pure PVA films, or of PVA films doped with various agents, is implant coating. In the case of metallic medical implants (e.g., titanium and titanium alloys that are permanently placed in the body), proper integration between the bone and the implant is of great concern. Metallic materials usually have poor osseointegration, and this reduces the endurance of metallic implants [46]. The abundant hydroxyl groups on PVA can be readily modified to attach growth factors and adhesion proteins [47]. Mahmoudi et al. reported that PVA-coated iron oxide nanoparticles demonstrated acceptable levels of cell viability, with none of them demonstrating toxic effects at the concentrations tested [48]. Beneficial properties of gold, such as good biocompatibility, and excellent resistance to oxidation and acids, promote the applicability of gold nanoparticles in nanomedicine or antibacterial applications [49,50]. On the PVA films containing five-branched gold nanostars (synthesized via a seed-growth method), the eradication of bacteria growth was determined after a laser-induced increase in surface temperature [51]. Using combination of poly(ethylene glycol) (PEG) and Au nanoparticles in hydrogels increased the wound healing efficiency due to the re-epithelization effect and collagen formation [52].

PVA-based materials may be used for the direct creation of medical implants. In some tissue replacements, e.g., intervertebral discs, the implant is a solid PVA hydrogel having a unitary body, which is shaped to correspond to a natural spinal disc. PVA powder crystals with molecular weight (MW) between about 124,000 and about 165,000, and with about 99.3%–100% hydrolysis, can be used to form a medical PVA hydrogel implant [53].

Currently, PVA is one of the most widely-used synthetic polymers in the form of wound covers or drug delivery systems. A pure PVA hydrogel does not achieve the elasticity and the hydrophilic character required for the polymer membranes used in the applications mentioned above. For this reason, doped PVA foils are produced, which incorporate natural polysaccharides, nanoparticles or other synthetic polymers into their structure [18]. In this study, we decided to optimize the process for preparing PVA hydrogels. Subsequently, we doped PVA foils with selected substances, namely (Cel), (PEG) or gold nanoparticles. Pristine foils and also doped foils were modified in plasma discharge in

order to improve their biocompatibility. The properties of PVA foils were then studied by a number of analytical methods, and their cytocompatibility was tested in cultures of human adipose tissue-derived stem cells (ASCs).

2. Materials and Methods

2.1. Material

Polyvinyl alcohol (PVA; 98%–99% hydrolyzed, MW = 89,000–98,000 g·mol^{−1}) from Alfa Aesar (Haverhill, MA, USA) was chosen for the preparation of the foils. Citric acid (monohydrate) was used as a crosslinking agent, and sulfuric acid (96%) was used to catalyze the reaction. The PVA foils were doped with: cellulose powder (Cel; Sigmacell cellulose, type 20 µm, Sigma Aldrich, St. Louise, MO, USA), poly(ethylene glycol) 600 (PEG; MW = 570–630 g·mol^{−1}, Sigma Aldrich, St. Louise, MO, USA) and sputtered gold nanoparticles (Au) in a PEG colloid solution (PEG/Au; preparation was carried out according to the procedures reported in an article by Slepicka et al. [54,55]; the time of sputtering was 300 s, the current was 30 mA, and the distance of the electrodes was 50 mm). The concentration of Au nanoparticles was 60 mg·L^{−1}, which corresponds to 0.36 mg in 6 mL PEG, and the Au nanoparticles were about 10 nm in size [55].

2.2. Preparation of PVA Foil

The solution-casting method was used for preparing the PVA or doped PVA foils. The preparation was based on an article by Mohanapriya et al. [42], but the amount of chemicals and the experimental conditions were optimized for the specific type of PVA that was used.

The dissolution temperature of the polymer was adjusted in the experiment. In addition, we investigated the optimal form of citric acid for use, and also whether it is preferable to use this acid in solid form or dissolved in water. The specific amount of sulfuric acid was added as the reaction catalyst was determined. Foils were prepared in which 1–40 drops (0.05–2 mL) of sulfuric acid were added. Optimization of the preparation of polymeric PVA foils and the specific preparation process is described in Topic 3.1.

2.3. Surface Modification

The surface of the pristine and doped PVA foils was modified in a diode plasma discharge using the Balzers SCD 050 device (Baltec, Switzerland) by DC Ar plasma. The plasma process parameters were: the Ar flow was set to 0.3 L·s^{−1}, the gas pressure was 10 Pa, the input power was 3 W, the electrode distance was 50 mm, and the time of modification was 120 s. Gas purity of 99.997% was used. The “top side” of the polymer was always modified, and this side of the polymeric material was not in contact with the poly(methyl methacrylate) (PMMA) casting plate. The surface parameters (especially the surface morphology and the surface roughness) of the prepared foils were therefore not affected by the PMMA casting plate.

2.4. Analytical Methods

The contact angle was determined by goniometry using a static water drop method. The measurements of the water contact angle were performed using distilled water (10 different positions) and the Surface Energy Evaluation System (SEE System, Advex Instruments, Brno, Czech Republic). The contact angle was measured during sample ageing for 50 days. The contact angle was first measured 1 h after the treatment.

The following analyses were performed on aged samples with a stabilized surface chemistry (30 days after surface modification). The elemental composition of the surface layer was proved by X-ray photoelectron spectroscopy (XPS), using an Omicron Nanotechnology ESCAProbeP spectrometer (Scienta Omicron, Taunusstein, Germany). The analyzed area was 2 mm × 3 mm. The X-ray source provided monochromatic radiation of 1485 eV. The spectra were measured stepwise, with a step in the

binding energy of 0.05 eV, and the take-off angle was 0° with respect to the surface normal. Spectrum evaluation was carried out by CasaXPS software. Characteristic C(1s), N(1s), O(1s), S(2p) and Au(4f) peaks were searched for. The concentration of the elements was given as an atomic percentage.

The surface morphology and the roughness of the pristine and doped foils was determined with the use of an atomic force microscope (AFM; Dimension ICON, Bruker Corp., Billerica, MA, USA); quantitative nanomechanical mapping (QNM) mode in air was used for the determination. A Silicon Tip on Nitride Lever SCANASYST-AIR (Bruker Corp., Billerica, MA, USA), with spring constant $0.4 \text{ N}\cdot\text{m}^{-1}$, was used. NanoScope Analysis software (version 1.8) was applied for data processing. The mean roughness values (R_a) represent the average of the deviations from the center plane of the sample.

The thickness of the foils was determined by laser confocal microscopy. For confocal microscopy, we used an Olympus LEXT OLS3100 device (Olympus Corp., Tokyo, Japan). For the laser confocal microscopy (LCM) analysis, we chose an Olympus LEXT OLS 3100 microscope with a blue laser ($\lambda = 407 \text{ nm}$) and with magnification up to 14,400×.

In practice, hydrogels are usually described by the swelling degree (Q), which determines the relative weight increase on swelling. The relative increase in weight of the PVA foils upon swelling was determined by gravimetric analysis. Three samples of each type of foil were subjected to the swelling test. The samples were weighed and were then immersed in a phosphate buffered saline (PBS) solution, in which they were left at room temperature for 24 or 48 h. The swollen samples were removed from the PBS solution after a specified period of time, were wiped with a paper towel to remove excess fluid from the foil surface, and were then weighed. The degree of swelling (Q) was calculated as follows: $Q = (m_\tau - m_0)/m_0$, where m_τ is the weight of a swollen sample determined 24 or 48 h after immersion of the sample in PBS, and m_0 is the weight of a dry sample.

The tensile test was performed on an Instron 3365 with pneumatic jaws without a strain gauge. The selected crosshead travel rate was 20 mm per min. Ten selected samples were cut for a selected representatives of doped foils. The results were then processed in Bluehill software (Bluehill 3). The Young's modulus of elasticity, the maximum stress, the elongation at maximum load, the tensile stress at failure and the elongation of the samples were obtained. Tensile tests were performed at room temperature.

2.5. Cell–Material Interaction—A Study of the Adhesion and Proliferation of the Cells

The cell–material interaction was studied in vitro using human adipose tissue-derived stem cells (ASCs) in order to determine the potential of our newly-developed materials as cell carriers for tissue engineering. The cells were isolated from lipoaspirates obtained by liposuction from a healthy female donor by a procedure earlier described in a study by Travnickova et al. [56]. The isolation of the cells was performed in compliance with the Declaration of Helsinki, under ethical approval from the Ethics Committee at Na Bulovce Hospital in Prague, and after written informed consent of the patient. In the 2nd passage, the cells were characterized by flow cytometry for the presence of stem cell-specific markers, such as CD105, CD90, CD73, CD29, and for the absence of endothelial and hematopoietic cell markers, such as CD45, CD34 and CD31 (CD—cluster of differentiation) [56].

The material samples were sterilized for 1 h in 70% ethanol, were inserted into 12-well plates (TPP, Trasadingen, Switzerland), and were fixed to the well bottom with plastic rings. The cells were seeded on the samples at a density of 16,000 cells per cm^2 into 3 mL of Dulbecco's Modified Eagle Minimum Essential Medium (DMEM, Sigma Aldrich, St. Louis, MO, USA, Cat. No. D5648) containing 10% fetal bovine serum (FBS; Gibco, Thermo Fisher Scientific, Waltham, MA, USA), 10 ng mL^{-1} of recombinant human fibroblast growth factor basic (FGF2; GenScript, Piscataway, NJ, USA) and 40 $\mu\text{g mL}^{-1}$ of gentamicin (LEK, Ljubljana, Slovenia). The cells were cultivated on the samples for 1, 3 and 6 days at a temperature of 37 °C, humidity of 85% and in an air atmosphere containing 5% CO_2 .

The viability of the cultivated cells that had been trypsinized from the samples was measured on a Vi-CELL XR (Beckman Coulter, Brea, CA, USA), using the trypan blue exclusion method. In order to

visualize the cells on the samples, the cells were fixed with 70% ethanol for 10 min and were stained for 1 h at room temperature with a mixture of Hoechst 33258 ($10 \mu\text{g mL}^{-1}$, Sigma-Aldrich, St. Louise, MO, USA), which stains the cell nuclei, and of Texas Red C2-maleimide ($1.7 \mu\text{g mL}^{-1}$, Invitrogen, Carlsbad, CA, USA), which stains the proteins of the cell membrane and cytoplasm. The number and the morphology of the cells on the sample surface were then evaluated on microphotographs taken under an Olympus IX 51 microscope (Olympus Corp., Tokyo, Japan) (objective 20 \times , 20 randomly distributed images for each sample, visualized area of 0.136 mm^2), equipped with an Olympus DP 70 digital camera. The number of cells was determined using NIS-Elements AR 3.0 image analysis software (Nikon Imaging Software - Advanced Research, version 3.0) on days 1, 3 and 6 after seeding. Statistically significant differences between the data acquired for each type of tested samples were analyzed by Excel, using XLSTAT software: one-way ANOVA (analysis of variance). All tests were performed with a confidence interval of 0.95. Statistically significant differences were observed in terms of groups ($p < 0.0001$).

3. Results and Discussion

3.1. Optimizing the Preparation Conditions of the PVA Foil

The process for preparing the PVA foils, mentioned in an earlier article dealing with the application of PVA for cell scaffolds, is relatively unspecified [42]. In order to optimize the preparation of the PVA foils, it was necessary to adjust the process and to identify the specific concentration of the substances that were used. For complete dissolution of the PVA, it was found that it is necessary to raise the temperature to 77°C . In order to determine a suitable form of the citric acid that was used, foils with comparable properties were prepared. If the citric acid was used as an aqueous solution, the excess water had to be evaporated. The amount of evaporated water was very difficult to detect. For the sake of simplicity, we therefore chose to use citric acid in the solid form. A specific amount of sulfuric acid was added as the reaction catalyst. Foils were prepared in which 1, 2, 5, 10, 15, 20, 25, 30, 35 and 40 drops of sulfuric acid were added. The foils containing 30, 35 and 40 drops of sulfuric acid were evaluated as optimal. Foils with smaller amounts were not sufficiently cross-linked. The foils were flexible, solid, transparent, and did not dissolve in water at room temperature or at an elevated temperature (77°C). Specific instructions for preparing individual types of PVA foils are given below. The preparation of “pristine” PVA foils involved dissolving 6 g of PVA in 150 mL of distilled water for 1 h at 77°C (with mechanical stirring at a rate of 600 rpm) until a clear solution was obtained. Subsequently, 0.6 g of citric acid and 30 drops (1.5 mL) of sulfuric acid were added to the solution. Then, the solution was stirred (for 1 h at 77°C , 600 rpm) to complete the crosslinking reaction. The viscous solution was cast into a PMMA mold (area 956 cm^2). Due to evaporation of the solvent and drying of the foil, the “solution” was kept at room temperature for 2 days.

The doped foils were prepared by adding specific substances (Cel, PEG or PEG/Au) into the PVA solution after the crosslinking substances had been added. The solution was subsequently stirred until the dopants were completely dissolved and the solution was homogenized. Then, the preparation of the doped foils continued as in the case of the “pristine” PVA foils.

3.2. Characterization of Pristine and Modified PVA Foils

3.2.1. Surface Wettability

It is known that plasma modification changes the surface properties of polymers. The surface wettability, the chemical composition and other properties may also change over a period of time, the so-called ageing time. Precise knowledge of the time needed to stabilize the surface of a sample is important for its applications and for the possibility of making subsequent material modifications. In addition, it is important in the correction of further analyses. Based on experience from our previous

experiments, where the samples were modified by plasma discharge, we assumed that the samples would age no more than 20 days after the modification [35,57].

The dependence of the contact angle of pristine PVA foils and of PVA foils doped with Cel, PEG and PEG/Au on the time passing from plasma modification (i.e., the ageing time) is shown in Figure 1. The contact angle values of non-doped and doped PVA foils, either untreated or treated with plasma, are given in Table 1. It is evident that the samples can be divided into two groups.

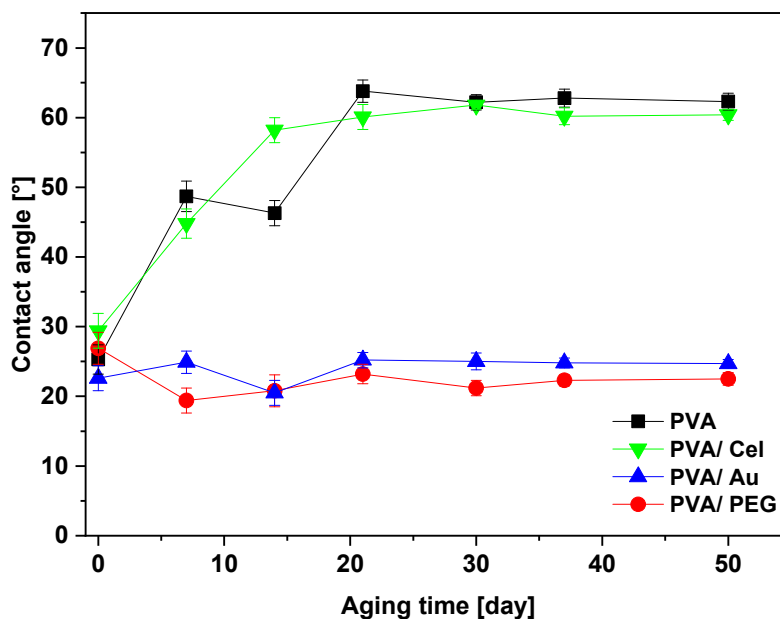


Figure 1. Ageing. Dependence of the water contact angle of plasma-treated PVA foils on the ageing time. The plasma-treated foils were either non-doped (PVA) or were doped with cellulose (PVA/Cel), with poly(ethylene glycol) (PVA/PEG) or with Au nanoparticles in a PEG colloid solution (PVA/Au).

Table 1. Values of the contact angles of PVA foils non-treated or treated with plasma and aged for 30 days. The foils were either non-doped (PVA) or were doped with cellulose (PVA/Cel), with poly(ethylene glycol) (PVA/PEG) or with Au nanoparticles in a PEG colloid solution (PVA/Au).

Sample	Contact Angle (°)			
	PVA	PVA/Cel	PVA/PEG	PVA/Au
Plasma-untreated	71.7 ± 1.3	73.1 ± 1.7	28.0 ± 1.4	24.3 ± 1.6
Plasma-treated/aged	62.3 ± 1.2	60.4 ± 0.8	22.5 ± 0.9	24.7 ± 0.6

(i) The first group consists of PVA and PVA/Cel foils, where the contact angle values of the plasma-untreated samples are high (more than 70°), and then these values decrease significantly immediately after plasma treatment. During the subsequent ageing process, the contact angle in this group increases again, and 21 days after modification it reaches the maximum values. The reaction of the plasma-treated polymeric surface with oxygen from the ambient atmosphere after treatment leads to the formation of oxygen-containing polar groups on the polymer surface. The increase in the contact angle values is caused by rearrangement of the oxygen-containing groups into the polymer volume.

(ii) The second group consists of PVA/PEG and PVA/Au. The contact angles of these polymeric foils are much lower, and are much less changed than PVA and PVA/Cel by plasma modification. This can be due to the fact that the pristine PVA contains a very small amount of oxygen, and PEG or PEG/Au doping to the polymer enabled us to introduce an “extreme” amount of polar groups into the polymer volume and onto the polymer surface. The surface hydrophilicity of the material was therefore increased.

3.2.2. Chemical Composition

The surface chemistry of the pristine and plasma-treated PVA and of the doped PVA was studied using XPS elemental composition analysis. The presence of carbon, oxygen, nitrogen, sulfur and gold atoms in the PVA and doped PVA surface layers is shown in Table 2. It was confirmed that plasma modification changed the chemical composition of the surface layers. An XPS analysis revealed that the PVA foils and the PVA/Cel foils contain less oxygen than PVA doped with PEG or with Au. We have confirmed that plasma treatment induced oxygen-containing groups on the material surface, so that the amount of elemental oxygen detected by the XPS method increased for all studied polymeric foils. The presence of nitrogen atoms was also detected on the top surface of the plasma-treated samples. This may be due to the reaction mentioned above, where the radical sites induced by the plasma activation serve as active binding sites for the reaction with nitrogen from the surrounding atmosphere.

Table 2. Atomic concentrations of selected elements C(1s), O(1s), N(1s), S(2p) and Au(4f) measured by XPS in PVA foils non-treated or treated with plasma, which were either non-doped (PVA) or were doped with cellulose (PVA/Cel), with poly(ethylene glycol) (PVA/PEG) or with Au nanoparticles in a PEG colloid solution (PVA/Au).

Sample	Atomic Concentrations (at.%)				
	C(1s)	O(1s)	N(1s)	S(2p)	Au(4f)
PVA	75.6	22.4	–	2.0	–
PVA/plasma	69.6	28.0	0.2	2.2	–
PVA/Cel	73.3	24.3	–	2.4	–
PVA/Cel/plasma	69.0	27.1	1.7	2.2	–
PVA/PEG	68.6	29.1	–	2.3	–
PVA/PEG/plasma	65.2	32.3	0.6	1.9	–
PVA/Au	67.9	29.9	–	2.2	0.1
PVA/Au/plasma	66.3	31.5	0.4	1.7	0.1

The amount of oxygen in the material surface is often positively correlated with the wettability of the material surface. These results are consistent with the results obtained by the goniometric method. From the analysis of the Au(4f) peak, it was determined that the atomic concentration of gold was 0.1 at.% in the surface layers. Typical XPS spectra of pristine non-doped PVA and PVA doped with Au nanoparticles are shown in Figure 2.

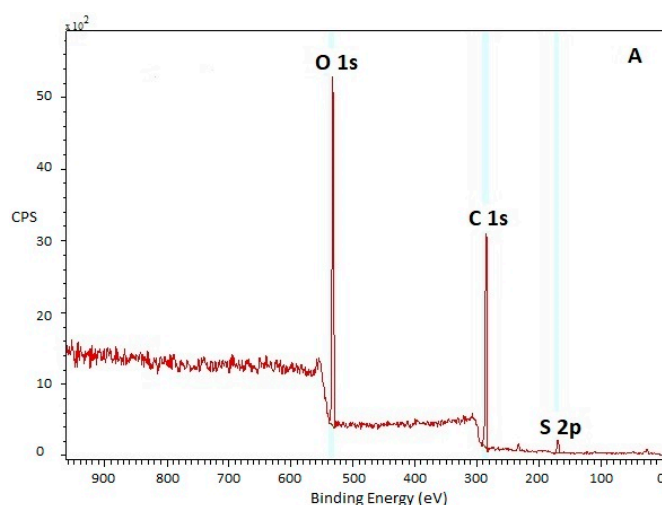


Figure 2. Cont.

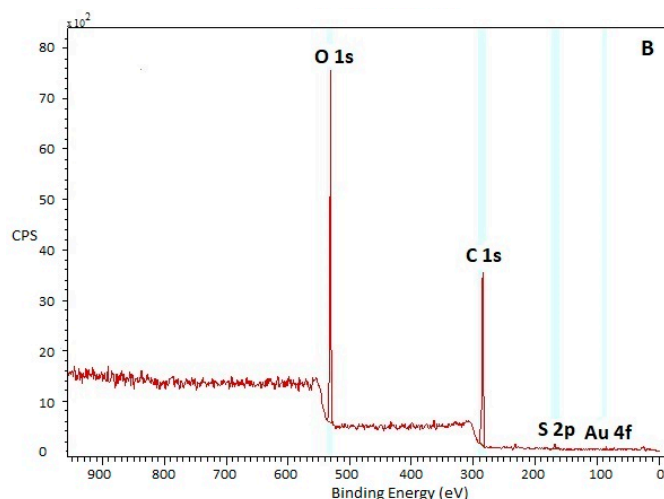


Figure 2. XPS spectrum of pristine PVA (A) and PVA doped with Au nanoparticles in a PEG colloid solution (B).

3.2.3. Surface Morphology and Roughness, Thickness of Samples

The thickness of the foils was determined using a confocal microscope. The thickness values were: for PVA $62.9 \pm 1.7 \mu\text{m}$, for PVA/PEG $112.5 \pm 1.6 \mu\text{m}$, for PVA/Au $151.4 \pm 2.3 \mu\text{m}$, and for PVA/Cel $126.2 \pm 2.8 \mu\text{m}$.

The surface morphology and the roughness of the pristine and doped PVA foils were studied using AFM. For comparison, we chose representative scans of an area of $10 \mu\text{m} \times 10 \mu\text{m}$, showing the “microstructure”, and of an area of $1 \mu\text{m} \times 1 \mu\text{m}$, showing the “nanostructure”. The scans of pristine PVA and doped PVA foils are presented in Figure 3. This figure shows that the surface morphology of all prepared samples is rather similar both at the “micro-scale” and at the “nano-scale”, the foils are homogeneous and there are no significant morphological deformations, which was our aim. The PVA/Au surface is more rugged, which corresponds to a larger effective surface area S.

The value for the surface roughness of PVA/Au is also significantly higher. The “microstructure” and the “nanostructure” of the plasma-treated non-doped and doped PVA samples are shown in Figure 4. By comparing Figures 3 and 4, we can conclude that the plasma treatment significantly affects the surface morphology of the non-doped foils and also of the doped foils. The $10 \mu\text{m} \times 10 \mu\text{m}$ scans show that the surface morphology of the individual samples varies significantly. Plasma treatment of the non-doped PVA does not lead to significant changes in the surface morphology. Modification of PVA/Cel in the plasma discharge causes the formation of spherical objects homogeneously distributed over the surface of the sample with corresponding surface roughness.

Both PVA/PEG samples and PVA/Au samples are PEG-doped, and their surfaces have a similar morphology. PEG has the strongest effect on the surface morphology, if the sample undergoes plasma modification, leading to the appearance of pronounced “depressions” and a huge increase in the surface roughness. Both PEG and PEG/Au samples exhibit a circular pattern on its surface. This pattern consists of smaller units for samples doped with Au nanoparticles in PEG, while larger circular areas were detected on sample doped with PEG only. These surface inhomogeneities are probably induced by changes in surface free energy (tension) during polymer foil formation, which induces local areas of inhomogeneity. Gold nanoclusters decrease this surface tension. Contrary to that, cellulose is only incorporated into the PVA matrix, thus the surface roughness is not changed significantly.

The $1 \mu\text{m} \times 1 \mu\text{m}$ scans show a rather different situation. If we analyze the scans of $1 \mu\text{m} \times 1 \mu\text{m}$, we can divide the samples into two groups according to their morphological similarity. PVA and PVA doped with cellulose have a very similar surface morphology. The entire surface of the samples is homogeneously and densely covered with uniform protrusions. In the case of PVA/Cel, the protrusions are higher, and the high roughness value (R_a for PVA/Cel is approximately 4 times higher than R_a

for PVA) is caused by the ablation of the crystalline phase of the PVA/Cel composite. The second group consists of PVA/PEG and PVA/Au. For this group, it can be concluded that the morphological formations are less dense on the surface than in the case of the PVA/Cel group.

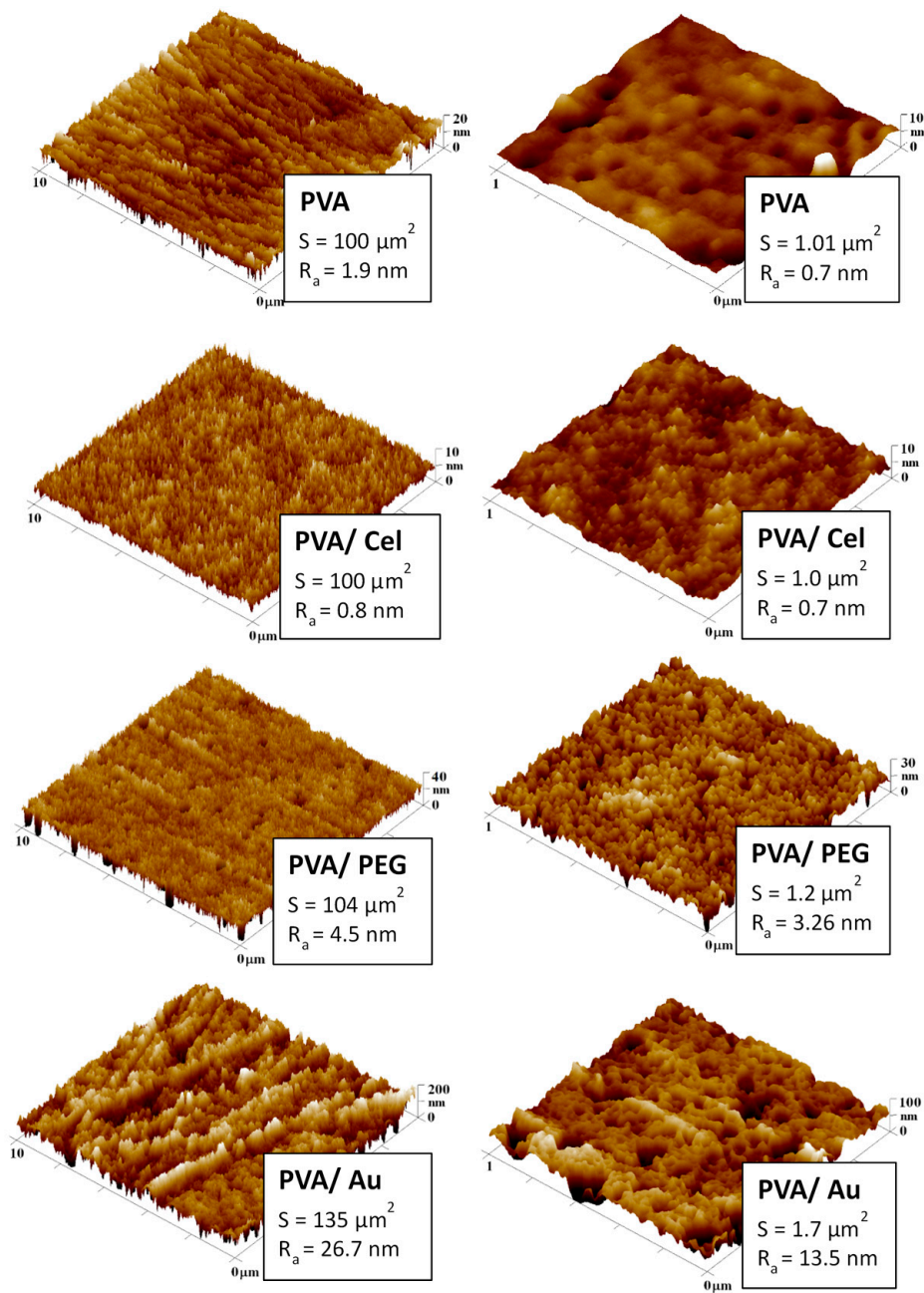


Figure 3. AFM images of pristine non-doped PVA and PVA doped with cellulose (PVA/Cel), poly(ethylene glycol) (PVA/PEG) and Au nanoparticles in a PEG colloid solution (PVA/Au). The column on the left column represents regions of $10 \mu\text{m} \times 10 \mu\text{m}$, and the column on the right represents regions of $1 \mu\text{m} \times 1 \mu\text{m}$. R_a is the average surface roughness in nm, S corresponds to the effective surface area.

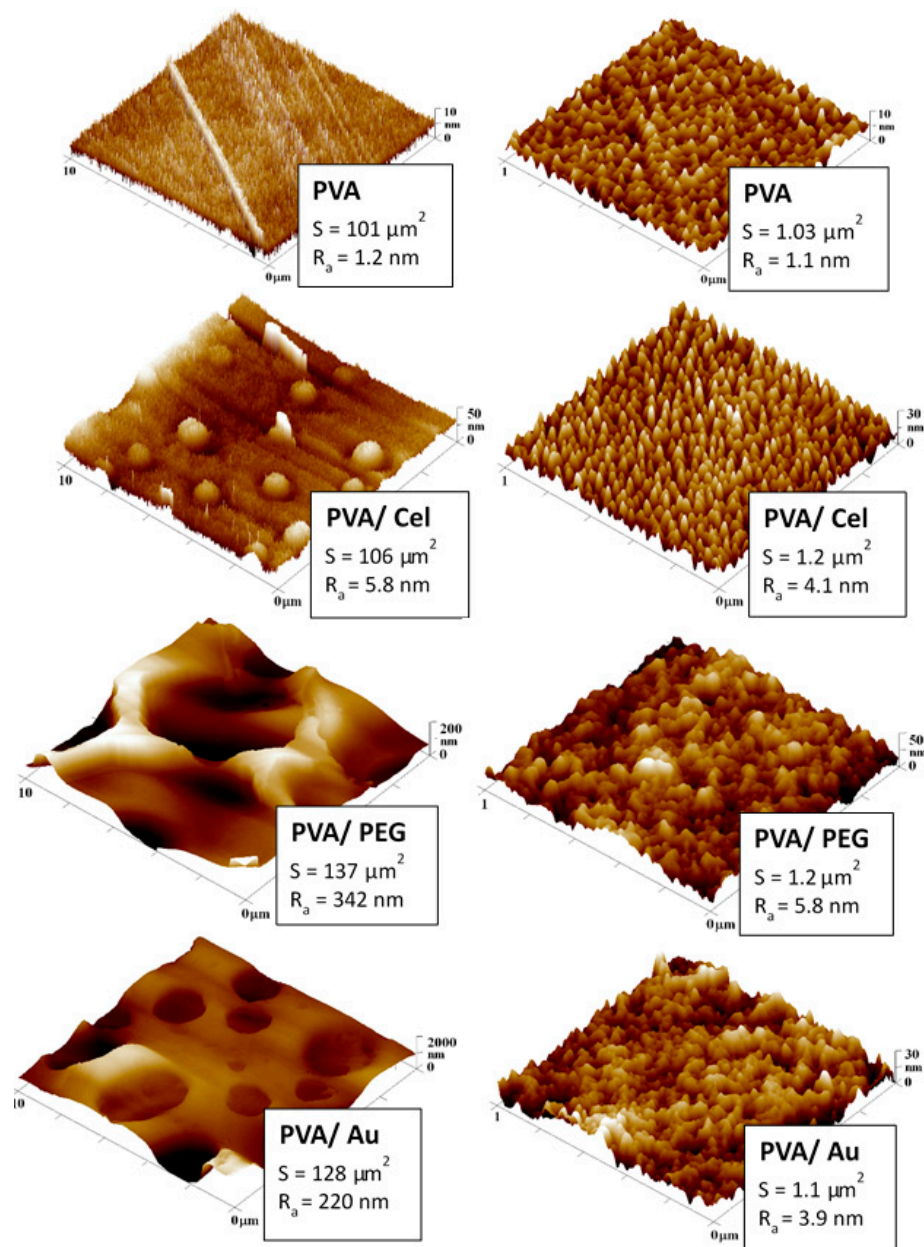


Figure 4. AFM images of plasma-treated PVA foils, which were either non-doped or were doped with cellulose (PVA/Cel), with poly(ethylene glycol) (PVA/PEG) or with Au nanoparticles in a colloid PEG solution (PVA/Au). The column on the left represents regions of $10\ \mu\text{m} \times 10\ \mu\text{m}$, and the column on the right represents regions of $1\ \mu\text{m} \times 1\ \mu\text{m}$. R_a is the average surface roughness in nm, S corresponds to the effective surface area.

3.2.4. Swelling

Hydrogels such as hydrophilic and polymeric networks are capable of absorbing large amounts of water. Doping PVA foils with various chemical substances and also various surface modifications leads to changes in swelling. If PVA foils are to be used as materials in the tissue engineering industry or in the pharmaceutical industry, it is necessary to control their swelling behavior.

The degree of swelling (Q) of individual samples in PBS was monitored for 24 and 48 h. Measurements taken after 48 h showed that the maximum degree of swelling was reached within the first 24 h. The Q values calculated according to the equation given in Section 2.4 are presented in

Table 3. We found that doping with cellulose does not affect the water absorption, as the swelling is the same for PVA and for PVA/Cel, whereas doping with PEG or Au nanoparticles into the PVA volume significantly increases the amount of liquid absorbed and thus the swelling of the foils. The cellulose chains are formed by microfibrils, which present crystalline ordering, disrupted by amorphous regions. The degree of crystallinity determines the amount of water resp. moisture that the cellulose is able to absorb. The higher the degree of crystallinity, the less hydroxyl groups available for the attachment of water molecules, and therefore the cellulose has a lower ability to water or absorb moisture [41]. For PEG-containing hydrogels, a network is formed whose mesh size is affected by the chain length of the PEG used. This space (eyes, pores, cavities) is filled with a liquid, which is referred to as a “free” liquid, after immersion of the sample in an aqueous medium. As the length of PEG used increases, the mesh size and thus the amount of absorbed fluid increases. After immersing the sample in water, disruption of the hydrogen bonding may also occur, causing repulsion between the polymer chains within the hydrogel, which led to an increase in the swelling ratio. The presence of PEG allows greater deformation of the polymer network of the hydrogel [58–60]. The experiment also shows that the samples not treated with plasma have greater swelling capacity than their plasma-modified versions. This may be due to the fact that plasma modification leads to ultraviolet light-induced crosslinking of polymers. Some information describing the possibility of crosslinking PVA by ultraviolet light of 254 nm can be found in [61].

Table 3. Degree of swelling of pristine non-doped PVA foils and of PVA foils doped with cellulose (PVA/Cel), with poly(ethylene glycol) (PVA/PEG) or with Au nanoparticles in a PEG colloid solution (PVA/Au), which were either untreated or were treated with plasma, and were immersed for 24 or 48 h in PBS.

Sample	Degree of Swelling	
	Q 24	Q 48
PVA	1	1.1
PVA/plasma	0.5	0.5
PVA/Cel	1	1
PVA/Cel/plasma	0.33	0.35
PVA/PEG	3	3
PVA/PEG/plasma	2	2
PVA/Au	3	3
PVA/Au/plasma	2.33	2.31

3.2.5. Mechanical Properties

The mechanical properties of selected foils were characterized by tensile tests, where the tested specimen was subjected to uniaxial tensile stress. The dependence of the elongation on the generated tensile stress was monitored by means of a deformation curve, which provided more detailed information about the strength characteristics of the samples. The following mechanical properties were investigated: the yield strength and the Young’s modulus, which defines the relationship between stress and strain in the material. Mechanical properties were determined from the deformation curve in the area, where Hook’s law applies. A linear dependence of the stress on the relative elongation, the elongation at yield point or the elongation at break corresponds to the relative permanent elongation of the specimen after breaking.

Table 4 shows that samples doped with PEG (i.e., PVA/PEG, PVA/Au), in their structure, exhibit higher values of Young’s modulus of elasticity and ductility than samples of PVA crosslinked with citric acid only. In the case of cellulose-doped foils, the values of these properties decreased slightly. The most significant changes were observed for PVA foil doped with PEG, where the strength of the foil was increased by the incorporation of PEG into the structure.

Table 4. Selected mechanical properties of the pristine PVA foils and of PVA foils doped with cellulose (PVACel), with poly(ethylene glycol) (PVA/PEG) or with Au nanoparticles in a PEG colloid solution (PVA/Au).

Sample	Mechanical Properties			
	Young's Modulus (MPa)	Ultimate Strength (MPa)	Elongation at Yield Strength (%)	Elongation at Break (%)
PVA	25.4 ± 3.7	12.4 ± 2.2	55.0 ± 10.0	63.0 ± 100.
PVA/Cel	26.1 ± 12.1	24.1 ± 3.9	135.0 ± 9.0	181.0 ± 22.0
PVA/PEG	197.9 ± 43.5	21.0 ± 1.9	162.0 ± 34.0	22 ± 22.0
PVA/Au	65.6 ± 18.4	17.2 ± 3.6	215.0 ± 47.0	302.0 ± 55

3.2.6. Biocompatibility

Human adipose-derived stem cells (ASCs) were used for studies of cell adhesion and growth on pristine or doped PVA foils, which were either untreated or were treated with plasma. The cell number was evaluated on the 1st, 3rd and 6th day after seeding. PVA foils doped with cellulose required careful handling; because after they were removed from a liquid (i.e., from 70% ethanol after sterilization or from PBS after rinsing), the shape of the samples changed (i.e., the samples were rolled into very tight beads). This made the samples difficult to handle and difficult to insert subsequently into the wells of culture plates. The number of initially-adhered cells (day 1) and the number of subsequently proliferating cells (days 3 and 6) on each substrate is shown in Figure 5. Tissue culture polystyrene (TCPS) was used as a control substrate.

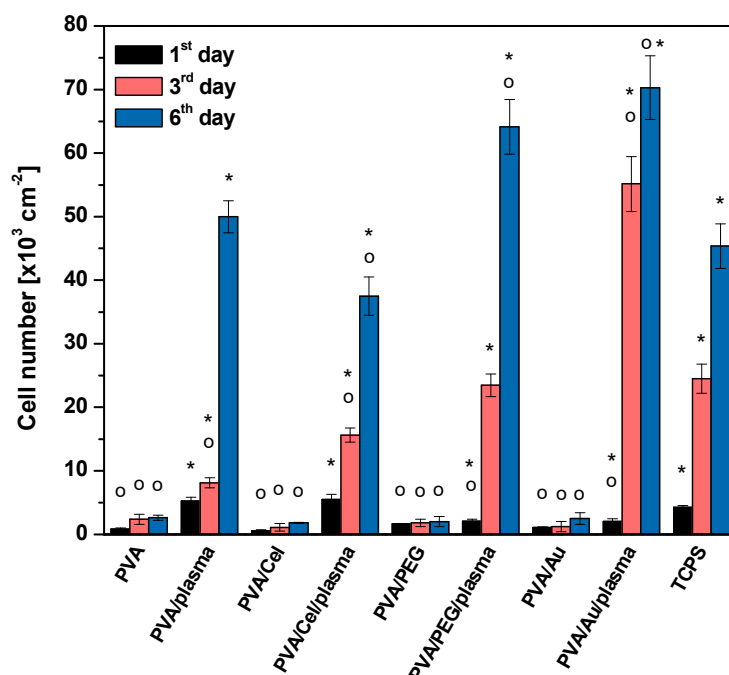


Figure 5. Number of human ASCs after initial adhesion (1st day) and subsequent proliferation (3rd and 6th day) on untreated and plasma-treated PVA foils either non-doped or doped with cellulose (Cel), with poly(ethylene glycol) (PEG) or with Au nanoparticles in a PEG colloid solution (Au), and on the control tissue culture polystyrene (TCPS). Statistical significance $p \leq 0.0001$ in comparison with TCPS (o) or the pristine PVA samples (*) is expressed using the ANOVA method (data were used from 40 images for each experimental group).

In this experiment, we observed significant improvement of the polymer cytocompatibility when plasma treatment was used. As shown in Figure 5, the plasma-treated samples produced more positive results than the untreated samples, and also more positive results than for the standard TCPS. Figure 5 shows that the samples untreated with plasma, including those modified with doping, exhibit minimal cell adhesion and proliferation during the cultivation period. The initial adhesion of cells to plasma-treated samples on day 1 was increased only in pristine PVA and in PVA doped with cellulose. However, on day 3 after seeding, the increase in the cell number on the plasma-treated PVA foils was markedly pronounced on all tested PVA samples. This increase continued up to day 6 after seeding, and was most pronounced on plasma-modified samples of PVA/PEG and PVA/Au. On day 6 after seeding, the final cell numbers on these samples were almost 1.5 times higher than on the control TCPS sample.

Figure 6 shows microphotographs of ASCs grown for 6 days on pristine and doped PVA foils, in plasma-untreated form and in plasma-treated form. The aim was to compare the cell spreading on the tested substrates with the cell spreading on TCPS. However, due to the high autofluorescence of PVA in the red channel, only cell nuclei stained in blue with Hoechst 33258 are visible on all PVA-based foils. The microphotographs show that the cells cultivated on the plasma-treated samples are homogeneously distributed throughout the test area, do not form clusters and are relatively numerous, while the cells are distributed very sparsely on the untreated samples. The trypan-blue exclusion test performed in cells cultured for 1, 3 or 6 days on the tested samples revealed that the viability of the cells on plasma-unmodified substrates was less than 10%. However, on plasma-modified substrates, this value rose above 90%. The viability of the cells cultured on TCPS was higher than 89%. This experiment demonstrated again a significant improvement of the polymer cytocompatibility when plasma treatment was used, and therefore it confirmed the results shown in Figure 5.

Interestingly, the most positive results on cell behavior were observed for plasma-treated PVA samples doped with PEG or with Au in PEG colloid solutions. This finding can be attributed to the highest content of oxygen and to the highest wettability of the plasma-treated PVA/PEG and PVA/Au samples (contact angle about 20° , Table 1). It is known that on wettable surfaces, the cell adhesion-mediating proteins from the serum supplement of the culture medium, such as vitronectin and fibronectin, are adsorbed in an active conformation that is well-accessible by cell adhesion receptors. This leads to improved cell adhesion and growth [34,35]. In accordance with this, the final cell number was relatively low on the plasma-treated PVA/Cel and PVA samples, which, after 21 days of ageing, displayed a relatively high contact angle (about 60°), indicating that they were relatively hydrophobic. In addition, the Young's modulus of these samples, especially in PVA/Cel, was lower than for the PVA/PEG and PVA/Au samples (Table 4). This could also, at least to some extent, hamper the cell growth. It has been reported that soft substrates with a low Young's modulus often cannot resist the traction forces generated by the adhering cells, and substrates of this type therefore disable proper cell spreading, which is a prerequisite for subsequent cell proliferation (for a review, see Ref. [11]).

Taken together, it is evident that the presence of a certain type of dopant in PVA foils can significantly influence the properties of these foils after plasma treatment, and also the subsequent behavior of cells on these foils. From this point of view, dopants in the form of PEG or Au in a colloid PEG solution seem to be most suitable for the use of PVA for tissue engineering, wound healing and other regenerative therapies.

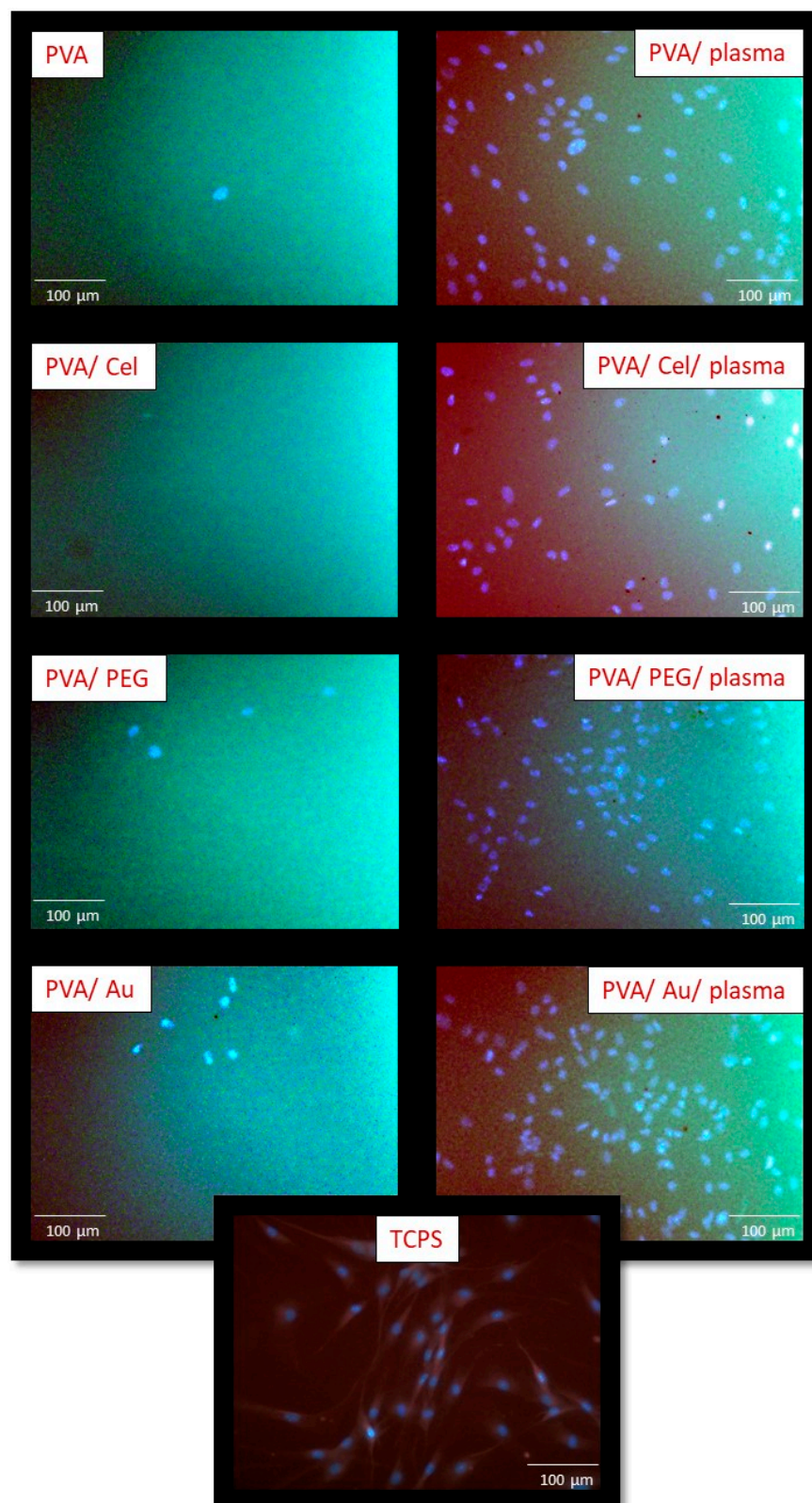


Figure 6. Fluorescence microscopy images of human ASCs on day 6 after seeding on untreated and plasma-treated PVA foils either non-doped or doped with cellulose (Cel), poly(ethylene glycol) (PEG) or with Au nanoparticles in PEG colloid solutions (Au), and on control tissue culture polystyrene (TCPS). Cell nuclei (blue) are stained with Hoechst 33258. All images have the same size and magnification.

4. Conclusions

We have optimized the process for preparing pristine and doped PVA hydrogels. PVA foils were doped with commercially available substances (cellulose powder, PEG) and also with Au nanoparticles prepared by sputtering to PEG colloid solutions. Prepared PVA and doped PVA foils were modified in an Ar plasma discharge to improve their physicochemical properties, their cytocompatibility and their suitability as a substrate for human adipose-derived stem cell cultivation.

We found that the plasma treatment affected and changed the wettability, the morphology, the chemical composition and the cytocompatibility of the surface. The goniometry determination showed significant changes in the water contact angle of plasma-treated PVA and PVA doped with cellulose during the ageing process. The changes observed for plasma-treated PVA doped with PEG or with Au nanoparticles were minimal in comparison with the non-treated foils. The XPS analysis determined an increase in the amount of oxygen for all plasma-modified samples. Plasma modification also confirmed the presence of nitrogen for selected samples. The plasma treatment of PVA and doped PVA foils induced ultraviolet crosslinking, which resulted in a decreased swelling value. The greatest decrease (65%–67%) was determined for the PVA sample doped with cellulose.

The main reason for using a plasma discharge for surface modification of PVA samples was to improve their cytocompatibility. The usefulness of this approach was confirmed by determining the number of adhered and subsequently proliferating cells and their viability. Only a minimal number of human adipose-derived stem cells was found on pristine non-doped or only doped samples, and their viability was very low. However, a dramatically large increase in the number of cultured cells was observed for the plasma-treated samples, especially on days 3 and 6 after seeding. In the case of PVA doped with PEG or with Au nanoparticles, a larger number of cells was determined on day 6 after seeding, even in comparison with TCPS.

The results of our study indicate that plasma-modified PVA foils, especially those doped with PEG and with Au in a colloid PEG solution, are promising candidates for application in regenerative medicine and in tissue engineering, due to their good mechanical and surface properties and their outstanding cytocompatibility. The plasma-treated samples can also be used as substrates for long-term cell culture for studies on the possibility of differentiating human adipose tissue-derived stem cells towards various cell types.

Author Contributions: Conceptualization, N.S.K.; methodology, N.S.K. and M.T.; validation, N.S.K. and P.S.; formal analysis, N.S.K., P.M., and B.I.; investigation, N.S.K.; resources, N.S.K. and B.I.; data curation, N.S.K. and V.Š.; writing—original draft preparation, N.S.K.; writing—review and editing, N.S.K. and P.S.; visualization, P.S.; supervision, V.Š. and L.B.; project administration, P.S., L.B., and V.Š.; funding acquisition, A.M. and P.S. All authors have read and agreed to the published version of the manuscript.

Funding: This research was funded by the Czech Science Foundation (Grant No. 19-02482S).

Conflicts of Interest: The authors declare no conflict of interest.

References

1. Menazea, A.A.; Mostafa, A.M.; Al-Ashkar, E.A. Effect of nanostructured metal oxides (CdO, Al₂O₃, Cu₂O) embedded in PVA via Nd:YAG pulsed laser ablation on their optical and structural properties. *J. Mol. Struct.* **2020**, *1203*, 1–7. [[CrossRef](#)]
2. Ratner, B.D.; Bryant, S.J. Biomaterials: Where we have been and where we are going. *Annu. Rev. Biomed. Eng.* **2004**, *6*, 41–78. [[CrossRef](#)] [[PubMed](#)]
3. O'Brien, F.J. Biomaterials & scaffolds for tissue engineering. *Mater. Today* **2011**, *14*, 88–95.
4. Deb, P.; Deoghare, A.B.; Borah, A.; Barua, E.; Lala, S.D. Scaffold development using biomaterials: A review. *Mater. Today Proc.* **2018**, *5*, 12909–12919. [[CrossRef](#)]
5. Caló, E.; Khutoryanskiy, V.V. Biomedical applications of hydrogels: A review of patents and commercial products. *Eur. Polym. J.* **2015**, *65*, 252–267. [[CrossRef](#)]
6. Hoffman, A.S. Hydrogels for biomedical applications. *Adv. Drug Deliv. Rev.* **2012**, *64*, 18–23. [[CrossRef](#)]

7. Coviello, T.; Matricardi, P.; Marianecchi, C.; Alhaique, F. Polysaccharide hydrogels for modified release formulations. *J. Control. Release* **2007**, *119*, 5–24. [[CrossRef](#)]
8. Ottenbrite, R.M. *Biomedical Applications of Hydrogels Handbook*; Ottenbrite, R.M., Park, K., Okano, T., Eds.; Springer Science: New York, NY, USA, 2010.
9. Premkumar, P.S. Preparation and electrical studies on pure and oxygen plasma treated polyvinyl alcohol films. *J. Mater. Res. Technol.* **2019**, *8*, 2232–2237. [[CrossRef](#)]
10. Ahmed, E.M. Hydrogel: Preparation, characterization, and applications: A review. *J. Adv. Res.* **2015**, *6*, 105–121. [[CrossRef](#)]
11. Discher, D.E.; Mooney, D.J.; Zandstra, P.W. Growth factors, matrices, and forces combine and control stem cells. *Science* **2009**, *324*, 1673–1677. [[CrossRef](#)]
12. Farida, O.; Mansour, F.; Habib, M.; Robinson, J.; Tarleton, S. Investigating the sorption influence of poly(vinyl alcohol) (PVA) at different crosslinking content. *J. Environ. Chem. Eng.* **2016**, *4*, 293–298. [[CrossRef](#)]
13. Raca, V.; Lević, S.; Balanč, B.; Graells, B.O.; Bijelić, G. PVA Cryogel as model hydrogel for iontophoretic transdermal drug delivery investigations. Comparison with PAA/PVA and PAA/PVP interpenetrating networks. *Colloid. Surf. B* **2019**, *180*, 441–448. [[CrossRef](#)] [[PubMed](#)]
14. Hoare, T.R.; Kohane, D.S. Hydrogels in drug delivery: Progress and challenges. *Polymer* **2008**, *49*, 1993–2007. [[CrossRef](#)]
15. Boateng, J.S.; Matthews, K.H.; Stevens, H.N.E.; Eccleston, G.M. Wound healing dressings and drug delivery systems: A review. *J. Pharm. Sci.* **2008**, *9*, 2892–2923. [[CrossRef](#)] [[PubMed](#)]
16. Kima, M.-S.; Oh, G.-W.; Jang, Y.-M.; Ko, S.-C.; Park, W.-S.; Choi, I.-W.; Kim, Y.-M.; Jung, W.-K. Antimicrobial hydrogels based on PVA and diphlorethohydroxycarmalol (DPHC) derived from brown alga *Ishige okamurae*: An in vitro and in vivo study for wound dressing application. *Mat. Sci. Eng. C Mater.* **2020**, *107*, 1–12.
17. Fang, H.; Wang, J.; Li, L.; Xu, L.; Wu, Y.; Wang, Y.; Fei, X.; Tian, J.; Li, Y. A novel high-strength poly(ionic liquid)/PVA hydrogel dressing for antibacterial applications. *Chem. Eng. J.* **2019**, *365*, 153–164. [[CrossRef](#)]
18. Kamoun, E.A.; Kenawy, E.-R.S.; Chen, X. A review on polymeric hydrogel membranes for wound dressing applications: PVA-based hydrogel dressings. *J. Adv. Res.* **2017**, *8*, 217–233. [[CrossRef](#)]
19. Goenka, S.; Sant, V.; Sant, S. Graphene based nanomaterials for drug delivery and tissue engineering. *J. Control. Release* **2014**, *173*, 75–88. [[CrossRef](#)]
20. Žáková, P.; Slepíčková Kasálková, N.; Kolská, Z.; Leitner, J.; Karpíšková, J.; Stibor, I.; Slepíčka, P.; Švorčík, V. Cytocompatibility of amine functionalized carbon nanoparticles grafted on polyethylene. *Mat. Sci. Eng. C Mater.* **2016**, *60*, 394–401. [[CrossRef](#)]
21. Slepíčka, P.; Malá, Z.; Rimpelová, S.; Švorčík, V. Antibacterial properties of modified biodegradable PHB non-woven fabric. *Mat. Sci. Eng. C Mater.* **2016**, *65*, 364–368. [[CrossRef](#)]
22. Motealleh, A.; Kehr, N.S. Nanocomposite hydrogels and their applications in tissue engineering. *Adv. Healthc. Mater.* **2017**, *6*, 1–19.
23. DeMerlis, C.C.; Schoneker, D.R. Review of the oral toxicity of polyvinyl alcohol (PVA). *Food Chem. Toxicol.* **2003**, *41*, 319–326. [[CrossRef](#)]
24. Thong, C.C.; Teo, D.C.L.; Ng, C.K. Application of polyvinyl alcohol (PVA) in cement-based composite materials: A review of its engineering properties and microstructure behavior. *Constr. Build. Mater.* **2016**, *107*, 172–180. [[CrossRef](#)]
25. Tong, R.; Zhao, Y.; Chen, M.; Peng, Y. Multimode interferometer based on no-core fiber with GQDs-PVA composite coating for relative humidity sensing. *Opt. Fiber Technol.* **2019**, *48*, 242–247. [[CrossRef](#)]
26. Baker, M.I.; Walsh, S.P.; Schwartz, Z.; Boyan, B.D. A review of polyvinyl alcohol and its uses in cartilage and orthopedic applications. *J. Biomed. Mater. Res. B* **2012**, *100B*, 1451–1457. [[CrossRef](#)] [[PubMed](#)]
27. Teodorescu, M.; Bercea, M.; Morariu, S. Biomaterials of PVA and PVP in medical and pharmaceutical applications: Perspectives and challenge. *Biotechnol. Adv.* **2019**, *37*, 109–131. [[CrossRef](#)] [[PubMed](#)]
28. Siegel, J.; Polívková, M.; Slepíčková Kasálková, N.; Kolská, Z.; Švorčík, V. Properties of silver nanostructure-coated PTFE and its biocompatibility. *Nanoscale Res. Lett.* **2013**, *8*, 1–10. [[CrossRef](#)]
29. Figueiredo, K.C.S.; Alves, T.L.M.; Borges, C.P. Poly(vinyl alcohol) films crosslinked by glutaraldehyde under mild conditions. *J. Appl. Polym. Sci.* **2009**, *111*, 3074–3080. [[CrossRef](#)]
30. Kim, K.-J.; Lee, S.-B.; Han, N.-W. Kinetics of crosslinking reaction of PVA membrane with glutaraldehyde. *Korean J. Chem. Eng.* **1994**, *11*, 41–47. [[CrossRef](#)]

31. Liu, Z.; Dong, Y.; Men, H.; Jiang, M.; Tong, J.; Zhou, J. Post-crosslinking modification of thermoplastic starch/PVA blend films by using sodium hexametaphosphate. *Carbohydr. Polym.* **2012**, *89*, 473–474. [\[CrossRef\]](#)
32. Han, B.; Li, J.; Chen, C.; Xu, C.; Wickramasinghe, S.R. Effects of degree of formaldehyde acetal treatment and maleic acid crosslinking on solubility and diffusivity of water in PVA membranes. *Chem. Eng. Res. Des.* **2003**, *81*, 1385–1392. [\[CrossRef\]](#)
33. Guo, R.; Hu, C.; Li, B.; Jiang, Z. Pervaporation separation of ethylene glycol/water mixtures through surface crosslinked PVA membranes: Coupling effect and separation performance analysis. *J. Membr. Sci.* **2007**, *289*, 191–198. [\[CrossRef\]](#)
34. Reznickova, A.; Novotna, Z.; Kolska, Z.; Slepickova Kasalkova, N.; Rimpelova, S.; Svorcik, V. Enhanced adherence of mouse fibroblast and vascular cells to plasma modified polyethylene. *Mat. Sci. Eng. C Mater.* **2015**, *52*, 259–266. [\[CrossRef\]](#) [\[PubMed\]](#)
35. Slepíčková Kasálková, N.; Slepíčka, P.; Bačáková, L.; Sajdl, P.; Švorčík, V. Biocompatibility of plasma nanostructured biopolymers. *Nucl. Instrum. Meth. B* **2013**, *307*, 642–646. [\[CrossRef\]](#)
36. Mishra, S.; Bajpai, R.; Katare, R.; Bajpai, A.K. Radiation induced crosslinking effect on semiinterpenetrating polymer networks of poly(vinyl alcohol). *Express Polym. Lett.* **2007**, *1*, 407–415. [\[CrossRef\]](#)
37. Simpson, R.L.; Nazhat, S.N.; Blaker, J.J.; Bismarck, A.; Hille, R.; Boccaccini, R.; Hansen, U.N.; Amisa, A.A. A comparative study of the effects of different bioactive fillers in PLGA matrix composites and their suitability as bone substitute materials: A thermo-mechanical and in vitro investigation. *J. Mech. Behav. Biomed. Mater.* **2015**, *50*, 277–289. [\[CrossRef\]](#)
38. Nawawi, W.M.F.W.; Lee, K.Y.; Kontturi, E.; Murphy, R.J.; Bismarck, A. Chitin nanopaper from mushroom extract: Natural composite of nanofibers and glucan from a single biobased source. *ACS Sustain. Chem. Eng.* **2019**, *7*, 6492–6496. [\[CrossRef\]](#)
39. Woodward, R.T.; Markoulidis, F.; De Luca, F.; Anthony, D.; Malko, D.; McDonald, T.; Shaffer, M.; Bismarck, A. Carbon foams from emulsion-templated reduced graphene oxide polymer composites: Electrodes for supercapacitor devices. *J. Mater. Chem. A* **2018**, *6*, 1840–1849. [\[CrossRef\]](#)
40. Kamoun, E.A.; Chen, X.; Eldin, M.S.M.; Kenawy, E.-R.S. Crosslinked poly(vinyl alcohol) hydrogels for wound dressing applications: A review of remarkably blended polymers. *Arab. J. Chem.* **2015**, *8*, 1–14. [\[CrossRef\]](#)
41. Benabbas, R.; Sanchez-Ballester, N.M.; Bataille, B.; Sharkawi, T.; Soulairol, I. Development and pharmaceutical performance of a novel co-processed excipient of alginic acid and microcrystalline cellulose. *Powder Technol.* **2021**, *378*, 576–584. [\[CrossRef\]](#)
42. Mohanapriya, S.; Raj, V. Tuning biological properties of poly (vinyl alcohol) with amino acids and studying its influence on osteoblastic cell adhesion. *Mat. Sci. Eng. C Mater.* **2018**, *86*, 70–82. [\[CrossRef\]](#) [\[PubMed\]](#)
43. Faxälv, L.; Ekblad, T.; Liedberg, B.; Lindahl, T. Blood compatibility of photografted hydrogel coatings. *Acta Biomater.* **2010**, *6*, 2599–2608. [\[CrossRef\]](#) [\[PubMed\]](#)
44. Liu, F.; Mishbak, H.; Bartolo, P. Hybrid polycaprolactone/hydrogel scaffold fabrication and in-process plasma treatment using PABS. *Int. J. Bioprint.* **2019**, *5*, 1–9.
45. Nitschke, M.; Zschoche, S.; Baier, A.; Simon, F.; Werner, C. Low pressure plasma immobilization of thin hydrogel films on polymer surfaces. *Surf. Coat. Technol.* **2004**, *185*, 120–125. [\[CrossRef\]](#)
46. Liang, C.; Wang, H.; Yang, J.; Cai, Y.; Hu, X.; Yang, Y.; Li, B.; Li, H.; Li, C.; Yang, X. Femtosecond laser-induced micropattern and Ca/P deposition on Ti implant surface and its acceleration on early osseointegration. *Appl. Mater. Interfaces* **2013**, *5*, 8179–8186. [\[CrossRef\]](#)
47. Abdal-hay, A.; Hussein, K.H.; Casettari, L.; Khalil, K.A.; Hamdy, A.S. Fabrication of novel high performance ductile poly(lactic acid) nanofiber scaffold coated with poly(vinyl alcohol) for tissue engineering applications. *Mat. Sci. Eng. C Mater.* **2016**, *60*, 143–150. [\[CrossRef\]](#)
48. Lee, P.-J.; Ho, C.-C.; Hwang, C.-S.; Ding, S.-J. Improved physicochemical properties and biocompatibility of stainless steel implants by PVA/ZrO₂-based composite coatings. *Surf. Coat. Technol.* **2014**, *258*, 374–380. [\[CrossRef\]](#)
49. Borzenkov, M.; Määttänen, A.; Ihalainen, P.; Collini, M.; Cabrini, E.; Dacarro, G.; Pallavicini, P.; Chirico, G. Photothermal effect of gold nanostar patterns inkjet-printed on coated paper substrates with different permeability. *Beilstein J. Nanotechnol.* **2016**, *7*, 1480–1485. [\[CrossRef\]](#)
50. Thoniyot, P.; Tan, M.J.; Karim, A.A.; Young, D.J.; Loh, X.J. Nanoparticle–hydrogel composites: Concept, design, and applications of these promising, multi-functional materials. *Adv. Sci.* **2015**, *2*, 1–13. [\[CrossRef\]](#)

51. Borzenkov, M.; Moros, M.; Tortiglione, C.; Bertoldi, S.; Contessi, N.; Faré, S.; Taglietti, A.; D'Agostino, A.; Pallavicini, P.; Collini, M.; et al. Fabrication of photothermally active poly(vinyl alcohol) films with gold nanostars for antibacterial applications. *Beilstein J. Nanotechnol.* **2018**, *9*, 2040–2048. [CrossRef]
52. Mahmoud, N.N.; Hikmat, S.; Ghith, D.A.; Hajeer, M.; Hamadneh, L.; Qattan, D.; Khalil, E.A. Gold nanoparticles loaded into polymeric hydrogel for wound healing in rats: Effect of nanoparticles' shape and surface modification. *Int. J. Pharm.* **2019**, *565*, 174–186. [CrossRef] [PubMed]
53. Denozieri, G.; Ku, D.N.; Carticept Medical, Inc. (Assignee) Methods of Producing PVA Hydrogel Implants and Related Devices. U.S. Patent No. 8,038,920 B2, 18 October 2011.
54. Slepíčka, P.; Příbyl, M.; Fajstavr, D.; Ulbrich, P.; Siegel, J.; Řezníčková, A.; Švorčík, V. Grafting of platinum nanostructures on biopolymer at elevated temperature. *Colloids Surf. A* **2018**, *546*, 316–325. [CrossRef]
55. Slepíčka, P.; Elashnikov, R.; Ulbrich, P.; Staszek, M.; Kolská, Z.; Švorčík, V. Stabilization of sputtered gold and silver nanoparticles in PEG colloid solution. *J. Nanopart. Res.* **2015**, *17*, 1–15. [CrossRef]
56. Travnickova, M.; Pajorova, J.; Zarubova, J.; Krocilova, N.; Molitor, M.; Bacakova, L. The Influence of Negative Pressure and of the Harvesting site on the characteristics of human adipose tissue-derived stromal cells from lipoaspirates. *Stem Cells Int.* **2020**, *2020*, 1–13. [CrossRef]
57. Slepíčková Kasálková, N.; Slepíčka, P.; Sajdl, P.; Švorčík, V. Surface changes of biopolymers PHB and PLLA induced by Ar⁺ plasma treatment and wet etching. *Nucl. Instrum. Meth. B* **2014**, *332*, 63–67. [CrossRef]
58. Yang, T. Mechanical and Swelling Properties of Hydrogels. Ph.D. Thesis, KTH Royal Institute of Technology, Stockholm, Sweden, 2012.
59. Anushree, D. Characterization of Polyethylene Glycol Hydrogels for Biomedical Applications. Master's Theses, Louisiana State University, Baton Rouge, LA, USA, 2007. Available online: https://digitalcommons.lsu.edu/gradschool_theses/3502 (accessed on 4 November 2020).
60. Kask, A.M. Degradable Poly(ethylene glycol) Hydrogels for 2D and 3D Cell Culture, Technical-Documents/Articles; SigmaAldrich.com. Available online: https://www.sigmaaldrich.com/technical-documents/articles/material-matters/degradable-polyethylene-glycol-hydrogels.html?gclid=EAIaIQobChMI1KcmkPnp7AIVQ-R3Ch3p1w-tEAMYASAAEgKLNvD_BwE (accessed on 4 November 2020).
61. Takakura, K.; Takayama, G.; Ukida, J. Ultraviolet-induced crosslinking of poly(vinyl alcohol) in the presence of sensitizers. *J. Appl. Polym. Sci.* **1965**, *9*, 3217–3224. [CrossRef]

Publisher's Note: MDPI stays neutral with regard to jurisdictional claims in published maps and institutional affiliations.



© 2020 by the authors. Licensee MDPI, Basel, Switzerland. This article is an open access article distributed under the terms and conditions of the Creative Commons Attribution (CC BY) license (<http://creativecommons.org/licenses/by/4.0/>).